Environmental Science & Technology

pubs.acs.org/est

Article

Effect of Microbial Biomass and Humic Acids on Abiotic and Biotic Magnetite Formation

Xiaohua Han, Elizabeth J. Tomaszewski, Julian Sorwat, Yongxin Pan, Andreas Kappler, and James M. Byrne*

Cite This: *Environ. Sci. Technol.* 2020, 54, 4121−4130

Read Online

ACCESS | Metrics & More | Article Recommendations | Supporting Information

ABSTRACT: Magnetite (Fe_3O_4) is an environmentally ubiquitous mixed-valent iron (Fe) mineral, which can form via biotic or abiotic transformation of Fe(III) (oxyhydr)oxides such as ferrihydrite (Fh). It is currently unclear whether environmentally relevant biogenic Fh from Fe(II)-oxidizing bacteria, containing cell-derived organic matter, can transform to magnetite. We compared abiotic and biotic transformation: (1) abiogenic Fh (aFh); (2) abiogenic Fh coprecipitated with humic acids (aFh-HA); (3) biogenic Fh produced by phototrophic Fe(II)-oxidizer *Rhodobacter ferrooxidans* SW2 (bFh); and (4) biogenic Fh treated with bleach to remove biogenic organic matter (bFh-bleach). Abiotic or biotic transformation of Fh was promoted by Fe_{aq}^{2+} or Fe(III)-reducing bacteria. Fe_{aq}^{2+}-catalyzed abiotic reaction with aFh and bFh-bleach led to complete transformation to magnetite. In contrast, aFh-HA only partially (68%) transformed to magnetite, and bFh (17%) transformed to goethite. We hypothesize that microbial biomass stabilized bFh against reaction with Fe_{aq}^{2+}. All four Fh substrates were transformed into magnetite during biotic reduction, suggesting that Fh remains bioavailable even when associated with microbial biomass. Additionally, there were poorly ordered magnetic components detected in the biogenic end products for aFh and aFh-HA. Nevertheless, abiotic transformation was much faster than biotic transformation, implying that initial Fe_{aq}^{2+} concentration, passivation of Fh, and/or sequestration of Fe(II) by bacterial cells and associated biomass play major roles in the rate of magnetite formation from Fh. These results improve our understanding of factors influencing secondary mineralization of Fh in the environment.

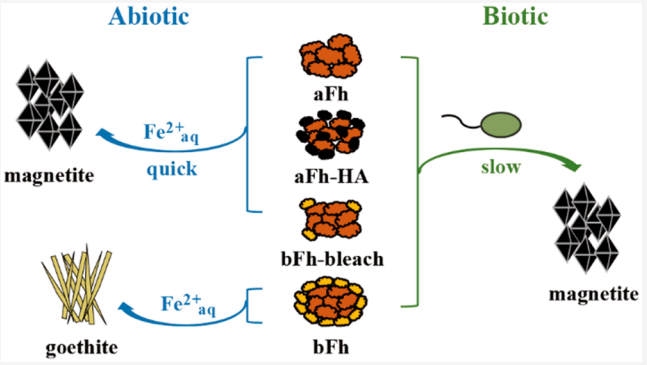

INTRODUCTION

Magnetite (Fe_3O_4), a mixed-valent magnetic mineral containing both Fe(II) and Fe(III) in a ratio of 1:2, is widespread in environments such as soils and sediments.[1] Magnetite is bioavailable, serving as an electron sink or electron source for Fe(II)-oxidizing and Fe(III)-reducing bacteria, respectively, contributing to biogeochemical cycling of Fe in terrestrial and aquatic environments.[2,3] Additionally, the unique properties of magnetite allow for its use in many diverse applications including medical treatments, carbon sequestration, and groundwater remediation.[4−6] Thus, understanding the formation mechanisms of magnetite in the environment is beneficial for understanding biogeochemical cycling of Fe and also for developing new bioinspired materials for industrial applications.

In natural environments, magnetite can be formed via abiotic or biotic mechanisms including biotic transformation of Fe(III) (oxyhydr)oxide minerals such as ferrihydrite (Fh).[2,7,8] Fe_{aq}^{2+} and dissimilatory Fe(III)-reducing bacteria can promote the transformation of Fh to magnetite or other crystalline ferric minerals, such as lepidocrocite (γ-FeOOH), goethite (α-FeOOH), or hematite (α-Fe_2O_3), depending on geochemical conditions (e.g., Fe_{aq}^{2+} concentration, pH, or the presence of ligands).[9−13]

In soil environments, Fh is often associated with natural organic matter (NOM), which is frequently approximated in laboratory studies by humic acids (HA), a chemically isolated subfraction of NOM.[8,14,15] Fh may be reduced by NOM either abiotically (via reduced functional groups present in NOM such as hydroquinones) or, more often, microbially by microorganisms using this organic matter as a carbon substrate.[16,17] Previous experiments studying the abiotic reduction of Fh containing adsorbed organic matter or coprecipitated with organic matter showed decreasing initial Fe(III) reduction rates and degrees of reduction with

Received: November 22, 2019
Revised: February 9, 2020
Accepted: March 4, 2020
Published: March 4, 2020

https://dx.doi.org/10.1021/acs.est.9b07095
Environ. Sci. Technol. 2020, 54, 4121−4130

increasing amounts of mineral-bound organic matter.[18−21] For biotic reduction of OM-Fh substrates, the effects of OM on Fh transformation to secondary phases depended on the extent OM acted as an electron shuttle for microbes and the extent of surface site blocking and/or aggregation.[22−24] In the environment, OM may also be associated with Fe minerals as a byproduct of Fe(II)-oxidizing bacteria, for example, photoferrotrophs which can harvest light energy and oxidize Fe(II) to Fe(III) (oxyhydr)oxides. This OM is usually associated with biogenic Fe(III) (oxyhydr)oxides (i.e., ferrihydrite) in oxygen-limited anoxic sediments, such as creeks, rhizospheres, and wetland systems.[25−28] The incorporation and/or surface aggregation of biomass can substantially impact mineral properties and transformation pathways of biogenic Fe(III) (oxyhydr)oxides.[20] However, little is known about the effects of microbial biomass on the reductive transformation pathways of biogenic Fe(III) (oxyhydr)oxides.

The main objective of this study was to assess the factors governing the rates and extent of abiotic and biotic reductive transformation of OM-ferrihydrite to magnetite in order to understand how such OM-mineral associations might influence biogeochemical Fe cycling in the environment. Here, we studied the abiotic and biotic transformation of abiogenic and biogenic Fh, with and without OM by Fe_{aq}^{2+} or Fe(III)-reducing bacteria *Shewanella oneidensis* MR-1, respectively. We monitored Fh transformation over time by following Fe redox speciation with the spectrophotometric ferrozine assay and magnetic susceptibility and analyzed the transformation products by Mössbauer spectroscopy.

MATERIALS AND METHODS

Preparation of Fh Substrates. Abiogenic ferrihydrite (aFh) was precipitated by the reaction of $Fe(NO_3)_3{\cdot}9H_2O$ (40 g) and KOH (1 M) until pH 7.5.[29] The material was centrifuged (7500 rpm; 10 min) and repeatedly washed three times with ultrapure H_2O (Milli-Q) to remove nitrate ions. Abiogenic ferrihydrite coprecipitated with HAs (aFh-HA) was synthesized following a similar approach as for aFh, except 3.26 g of HAs (Sigma-Aldrich, H16752) was added into $Fe(NO_3)_3{\cdot}9H_2O$ (40 g) before the addition of KOH (1 M). The mass of HA was chosen to ensure that the C/Fe ratio of aFh-HA matched that of bFh (see the Mineral Characterization section), which allows aFh-HA as more of an analogue to biogenic Fh using abiogenic synthesis procedures. Biogenic ferrihydrite (bFh) was produced from Fe(II) oxidation by the phototrophic Fe(II)-oxidizer *Rhodobacter ferrooxidans* SW2.[30] The mineral precipitate was centrifuged and repeatedly washed three times with ultrapure H_2O to remove ions and loosely associated bacteria from the medium. Organic matter-free biogenic ferrihydrite (bFh-bleach) was obtained by exposing bFh to 6% NaOCl to remove biogenic organic matter. This treatment was repeated up to six times, rolling at 40 rpm/min for 6 h during each treatment and decanting the supernatant solution after centrifugation.[31] The treated samples were washed with ultrapure H_2O to remove NaOCl. The Fe total concentration of all four starting materials was determined by chemical dissolution (1 M HCl), followed by the spectrophotometric ferrozine assay.[32]

Strains and Medium. Information about microbial strains and cultivation is provided in the Supporting Information.

Incubation Experiments. Abiotic experiments were performed in 50 mL serum bottles with 10 mM anoxic HEPES buffer, 3 mM Fh, and 7 mM $FeCl_2$. For biotic experiments, a cell suspension of *S. oneidensis* MR-1 with a cell concentration of 5×10^8 cells/mL was added to 10 mmol/L of Fh with 9 mM lactate as the electron donor in anoxic HEPES buffer (10 mM; pH 7.2). Triplicate experiments were used for Fe concentration quantification, and another set of triplicates were used for magnetic susceptibility (MS) measurements for each batch reactor. Separate bottles were required for MS because removal of the solid material for Fe quantification interferes with MS analysis. Control bottles containing no Fe_{aq}^{2+} or inoculum were included to confirm the absence of spontaneous transformation of Fh. All experiments were incubated at 28 °C in darkness. Figure S1 gives further details of all batch reactors with the four Fh substrates under abiotic and biotic reductive conditions.

Mineral Characterization. The specific surface area (SSA) of the four Fh substrates was determined by the Brunauer−Emmett−Teller method (Gemini VII Surface Area and Porosity Analyzer, Micromeritics, Germany). Fh substrates were analyzed by N_2 adsorption at 77 K after the samples were dried at 60 °C in an oven. For zeta potential (ZP) measurement, the four Fh substrates were diluted with 10 mM HEPES buffer, which was adjusted to pH 7.2 in order to have the same pH as in the initial medium. All measurements were conducted using a Zetasizer Nano ZSP with Zetasizer Nano Series disposable folded capillary cells (DTS1070; Malvern, Herrenberg, Germany). Total organic carbon (TOC) was quantified using a TOC analyzer (model 2100S, Analytik Jena, Germany) after the samples were dried at 60 °C in an oven. For Mössbauer analysis, samples of four Fh substrates and final mineral products were filtered on 0.45 μm filter papers and embedded in Kapton tape in a glovebox (100% N_2). These samples were stored in anoxic air-tight bottles at −20 °C until analysis. The samples were measured at 140 K using a ^{57}Fe Mössbauer spectrometer (WissEL) with a ^{57}Co/Rh source. Spectra were fitted using the Voigt-based fitting routine in the Recoil software (University of Ottawa).[33]

Fe Concentration Quantification and MS. Information about Fe concentration quantification and in situ volume-dependent MS measurements is provided in the Supporting Information.

Calculation of Delay between Fh Reduction and Magnetite Formation (Δt). In order to determine the differences between the increase in Fe(II)/Fe(III) ratio and increase in MS for the four Fh substrates in abiotic and biotic transformation experiments, the Fe(II)/Fe(III) and MS triplicate average values for individual batch reactors over time were fitted with the Hill equation (see the Supporting Information), with the first-order derivative calculated using Origin Pro 2017.

RESULTS

Ferrihydrite Substrate Properties. Mössbauer spectroscopy of all four Fh substrates at 140 K (Figure S2) was performed by doublets with hyperfine parameters that were indicative of ferrihydrite, with some potential interparticle interactions such as formation of larger aggregates because of HA and microbial biomass in samples aFh-HA and bFh.[19] C content, SSA, and ZP for ferrihydrite substrates are given in Table S1. TOC analyses revealed the C/Fe molar ratio of bFh and aFh-HA to be similar (0.39 and 0.42), while that of aFh and bFh-bleach was close to zero. The similarity of C/Fe and mineralogy of aFh and bFh-bleach suggest that the bleach (NaOCl) was successful at removing ∼97% biomass in bFh

https://dx.doi.org/10.1021/acs.est.9b07095
Environ. Sci. Technol. 2020, 54, 4121−4130

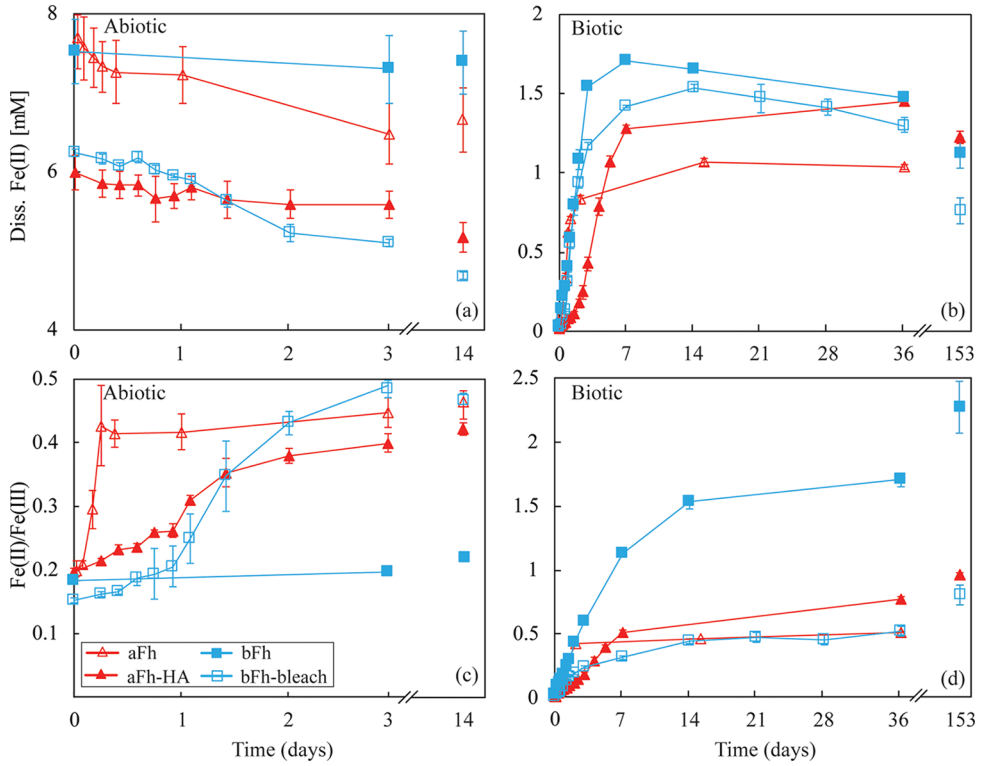

Figure 1. Ferrihydrite transformation promoted by Fe_{aq}^{2+} or Fe(III)-reducing bacteria *S. oneidensis* MR-1, respectively. (a,b) Fe_{aq}^{2+} concentration in abiotic and biotic transformations of ferrihydrite; (c,d) Solid-phase Fe(II)/Fe(III) ratios over time in abiotic and biotic transformation of ferrihydrite. Error bars indicate the range of triplicate culture bottles. Bars that are not visible are smaller than the symbols. Note the different time scales for abiotic and biotic batch reactors.

without affecting the mineralogical phase, although this cannot be fully confirmed without a more thorough analysis using high-resolution methods (e.g., high-resolution transmission electron microscopy) which fall beyond the scope of this study. Because of the blockage of mineral surface sites by HA, as well as the formation of larger aggregates, aFh-HA had much lower SSA, 13 m^2/g, compared to aFh (306 m^2/g). Similarly, the surface charge for aFh-HA was negative at −21.7 mV, while that of aFh was positive with +12.7 mV. The surface charge for bFh was also negative with −27.0 mV because of the presence of biomass. However, although the C/Fe molar ratios of bFh and aFh-HA were similar, the SSA of bFh (228 m^2/g) was not as low as that of aFh-HA, which implies that the extent of mineral surface site blockage by biomass and/or formation of aggregates was lower for bFh than for aFh-HA. Given that NaOCl removed ∼97% biomass in bFh, the bFh-bleach had slightly higher SSA (255 m^2/g) than bFh and a more positive surface charge with +2.60 mV.

Fh Reduction and Transformation over Time. Variations of Fe_{aq}^{2+} for both abiotic and biotic transformation of the four Fh substrates as well as the variations of the solid-phase Fe(II)/Fe(III) ratio of abiotic and biotic transformation are shown in Figure 1. The solid-phase Fe(II)/Fe(III) ratio was the ratio between total Fe(II) (including structural Fe(II) and adsorbed Fe(II)) and total Fe(III) (including structural Fe(III) and adsorbed Fe(III)), which was determined by the spectrophotometric ferrozine assay. No Fe^{3+}_{aq} was detected in any experiment. Detailed data are included in the Supporting Information.

In the abiotic transformation experiment, Fe_{aq}^{2+} decreased over time, likely because of adsorption and reaction with Fh. The Fe(II)/Fe(III) ratios at the first measured time point (0.5 h) for all four Fh substrates were ∼0.2 (i.e., not zero), suggesting the adsorption of Fe_{aq}^{2+}. The Fe(II)/Fe(III) ratio of aFh rapidly increased to 0.43 over 6 h and more slowly to 0.46 over 14 days. Compared with aFh, the Fe(II)/Fe(III) ratio of aFh-HA and bFh-bleach increased more slowly to 0.42 and 0.47 in 14 days, respectively. Conversely, the Fe(II)/Fe(III) ratio for bFh only increased by 0.08 in 56 days, even though some Fe_{aq}^{2+} was adsorbed to the mineral surface at the beginning of the experiment.

In the biotic transformation experiments, the Fe_{aq}^{2+} concentration in batch reactors containing aFh-HA, bFh, and bFh-bleach was higher (1.3−1.47 mM) than that with aFh (1.03 mM) after 36 days. This is likely due to the fact that Fe_{aq}^{2+} produced in these batch reactors could not react with Fh either because of surface site blockage by HA or biomass or potentially because of changes to the surface reactivity of bFh-bleach during bleach treatment, which were not detectable via Mössbauer spectroscopy. However, after 153 days, there were decreases of Fe_{aq}^{2+}, indicating that Fe(II) produced by *S. oneidensis* adsorbed to and reacted with Fh. The Fe(II)/Fe(III) ratio of aFh increased rapidly to 0.43 over 52 h and kept increasing more slowly to 0.52 over 36 days. Compared with aFh, the Fe(II)/Fe(III) ratio of aFh-HA and bFh-bleach increased more slowly reaching 0.52 in 7 days and 0.45 in 14 days, respectively, and kept increasing to 0.96 and 0.81 over 153 days. The Fe(II)/Fe(III) ratio of bFh continuously increased to 2.28 in 153 days. Only Fe(II)/Fe(III) of aFh was close to the stoichiometric magnetite ratio of 0.5, while the other three Fh substrates showed much higher values (0.96 for aFh-HA, 2.28 for bFh, and 0.81 for bFh-bleach), suggesting

https://dx.doi.org/10.1021/acs.est.9b07095
Environ. Sci. Technol. 2020, 54, 4121−4130

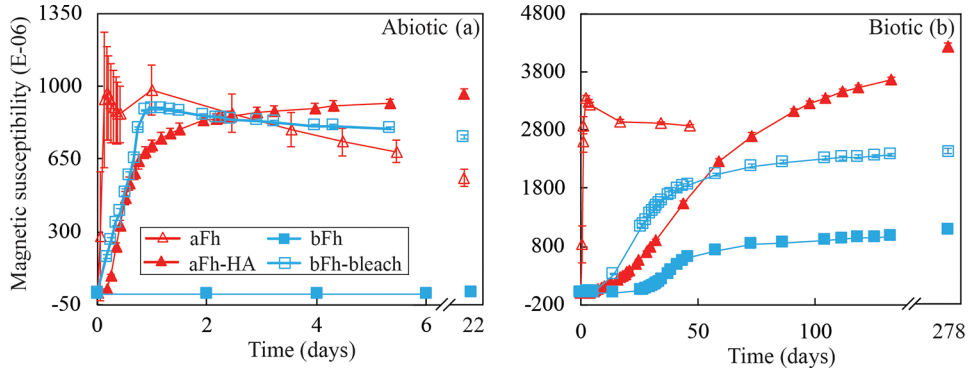

Figure 2. MS over time in abiotic (a) and biotic (b) transformation of ferrihydrite. Error bars indicate the range of triplicate culture bottles. Bars that are not visible are smaller than the symbols. Note the different time scales for the abiotic and biotic batch reactors.

that magnetite might not have been the only transformation product.

MS results for abiotic and biotic transformation are shown in Figure 2. Changes to MS in the experimental batch reactors matched expected changes based on Fe_{aq}^{2+} concentrations and Fe(II)/Fe(III) ratios described above. A previous study on in situ MS measurements showed MS measurements to be suitable for following microbial Fe(III) mineral transformation, in particular magnetite formation and transformation.[34] Given the composition of the media (only lactate and HEPES buffer were present), we expect that only the formation of ferrimagnetic magnetite will contribute to high increases in MS. Thermodynamically stable minerals goethite and hematite and the remaining paramagnetic minerals such as starting ferrihydrite have a much smaller, positive MS.

In abiotic experiments, the MS of aFh increased rapidly to 935×10^{-6} SI in only 3 h. The following decrease to 559×10^{-6} SI (43% decrease compared to the maximum MS) by day 22 likely indicates an increase of magnetite grain size. If some of the magnetite particles grow above the critical volume of the superparamagnetic to single domain transition, the overall MS value of the sample could decrease because of the lower MS of single domain particles compared to the smaller superparamagnetic grains.[35] Similarly, the MS of bFh-bleach increased rapidly to 896×10^{-6} SI in 1 day, followed by a decrease to 755×10^{-6} SI by day 22 (16% decrease compared to maximum MS). For aFh-HA, MS increased to 834×10^{-6} SI in 2 days and continued to slowly increase to 963×10^{-6} SI over 22 days. However, there was no MS change of bFh during 64 days, which is consistent with the Fe(II)/Fe(III) ratio of bFh, implying that microbial biomass present in bFh blocked the reaction between bFh and Fe_{aq}^{2+}.

In biotic Fh reduction experiments, the MS of aFh increased rapidly to 3345×10^{-6} SI in 2 days and decreased to 2871×10^{-6} SI (14% decrease compared to the maximum MS) after 47 days, similar to aFh in the abiotic experiment. Increasing trends of MS for aFh-HA, bFh, and bFh-bleach were similar, in which MS increased quickly in the first 133 days and kept increasing slowly until 278 days. The final MS value of bFh (1070×10^{-6} SI) in the biotic transformation experiment was similar to that of the other three Fh substrates in abiotic transformation, which owing to the fact that the final Fe(III) concentrations in the solid phase were also similar (2.8 ± 0.2 mM) suggests that a similar amount of magnetite was likely produced. The final MS values of aFh, aFh-HA, and bFh-bleach were higher (2871×10^{-6}, 4222×10^{-6}, and 2441×10^{-6} SI, respectively) than that of bFh in biotic transformation and had correspondingly higher final solid Fe(III) (3.4–4.6 mM).

Identity of Fh Transformation Products. 140 K Mössbauer spectra of transformation products are shown in Figure 3, with corresponding fit parameters presented in Table S2. Our data showed that the solid-phase products formed during Fe(II)-catalyzed abiotic transformation and during dissimilatory iron reduction of ferrihydrite by *S. oneidensis* MR-1 were goethite and magnetite, sometimes associated with a strong Fe(II) doublet in Mössbauer spectra, whose identity cannot be accurately determined but likely corresponds to Fe(II) adsorbed to the mineral surface. Some spectra also required the inclusion of a poorly ordered magnetic phase. This phase potentially represents either superparamagnetic magnetite or goethite which has not undergone full magnetic ordering at 140 K. The Fe(II)-catalyzed abiotic transformation of aFh and bFh-bleach led to complete transformation to magnetite, which is consistent with the Fe concentration results for aFh and bFh-bleach where the solid-phase Fe(II)/Fe(III) ratios for both Fh were close to 0.5 which is the stoichiometric Fe(II)/Fe(III) ratio of magnetite. In contrast, aFh-HA only underwent partial transformation to magnetite (68.2%), with paramagnetic Fe(III) (28.5%) and Fe(II) (3.3%) remaining in the solids after 22 day cultivation. bFh underwent further transformation into more thermodynamically stable goethite (16.7%); however, no magnetite was produced within 64 days.

Conversely, all four Fh substrates were transformed into magnetite during biotic Fe(III) reduction, although not to completion. Evidence of the remaining Fh suggests that even though the HA and biomass-associated Fh are bioavailable, the organic matter still partially prevents the transformation of Fh to magnetite. The maximum transformation extent of Fh in the biotic experiment is 68.5% for the bFh-bleach phase. Although aFh had no organic matter, there was a lower relative abundance of magnetite (~62.3%) produced compared to bFh-bleach with paramagnetic Fe accounting for the remaining spectral area. For aFh-HA and bFh, nearly half of the Fe was present as magnetite at 49.9 and 56.1%, respectively.

The Fe(II)/Fe(III) ratio of each of the magnetite formation products was determined based on Mössbauer spectroscopy and is shown in Table S3.[36] The ratios varied between samples, with aFh-HA (biotic) having the lowest value of 0.33, suggesting that stoichiometric magnetite was not formed. In contrast, bFh-bleach (biotic) had the highest Fe(II)/Fe(III) ratio of 0.54, which suggests a relatively reduced magnetite. In the only two samples which converted completely to magnetite

https://dx.doi.org/10.1021/acs.est.9b07095
Environ. Sci. Technol. 2020, 54, 4121−4130

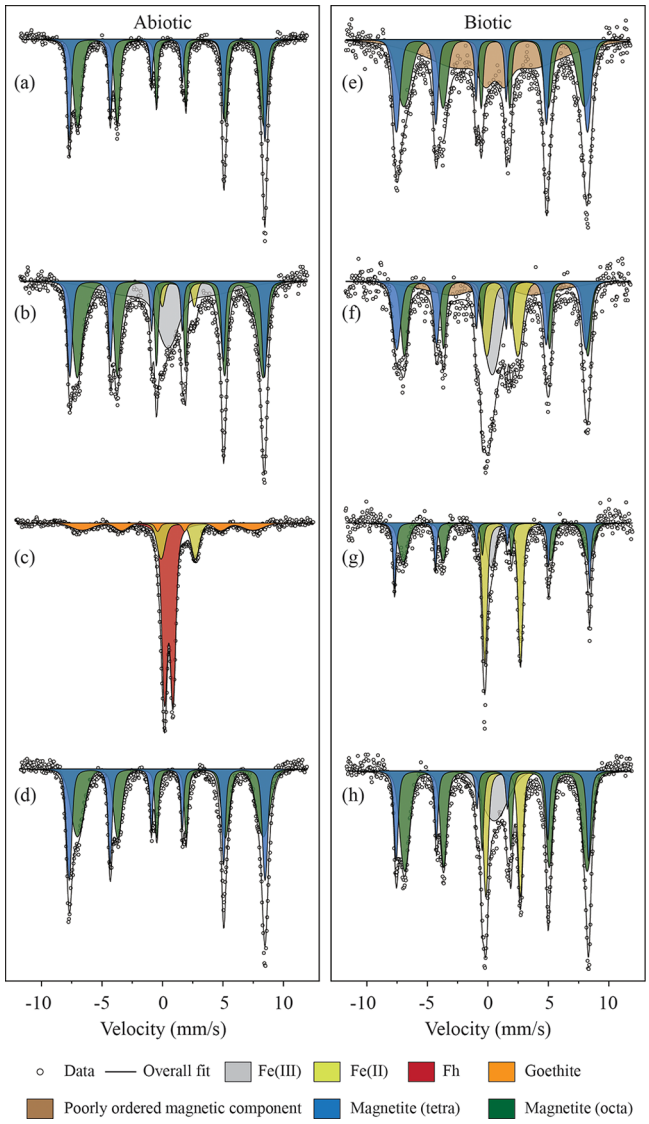

Figure 3. Mössbauer spectra of ferrihydrite transformation induced by Fe_{aq}^{2+} abiotically (a–d) and *S. oneidensis* MR-1 biotically (e–h). (a,e) aFh transformation products; (b,f) aFh-HA transformation products; (c,g) bFh transformation products; and (d,h) bFh-bleach transformation products. Open circles: measured data, solid line: fitted spectrum, filled areas: modeled relative amounts of identified minerals.

without any additional transformation products, the ratios were calculated to be 0.45 and 0.40 for aFh and bFh-bleach (abiotic), respectively. This suggests that magnetite formed from the bleach-washed biogenic ferrihydrite is partially oxidized in comparison to the pure ferrihydrite. However, no clear pattern emerged, which suggests that abiotic or biotic reactions favor either more reduced or more oxidized magnetite.

DISCUSSION

Role of Initial Fe_{aq}^{2+} Concentration and Fe(II)/Fh Ratio in Fh Transformation. Abiotic transformation was faster compared to biotic transformation, implying that the initial Fe_{aq}^{2+} plays one of the important roles in the rate of magnetite formation from Fh. Previous studies on Fe(II)-induced abiotic transformation of ferrihydrite showed that magnetite accumulation is only observed at Fe_{aq}^{2+} concentration exceeding 0.3 mM (equivalent to 0.5 mmol Fe[II]/g ferrihydrite), otherwise only lepidocrocite and/or goethite formed after 140 h[7,12] In our abiotic experiments, we cannot rule out the possibility that lepidocrocite and/or goethite formed as intermediate products. However, given that the Fe(II) concentration (Fe(II) to Fh ratio was 2.3, equivalent to 28 mmol Fe[II]/g ferrihydrite) and long duration of experiments (more than 510 h), such phases might have undergone transformation to magnetite and are thus not visible in the Mössbauer spectra. This initial Fe_{aq}^{2+} concentration was based on our abiotic preliminary experiments in which Fe_{aq}^{2+} was reacted with aFh at different Fe(II)/Fe(III) ratios (ranging from 0.5 to 10). In these preliminary experiments, MS results showed that no magnetite formed when the Fe(II)/Fe(III) ratio was 0.5 nor when the Fe(II)/Fe(III) ratio was 10 (Figure S3). Although the Fe(II)/Fe(III) ratio of 0.5 (equivalent to 6 mmol Fe[II]/g ferrihydrite) is higher than that required for magnetite nucleation,[7] the absence of any increase of MS implied that no magnetite was produced. Therefore, we speculate that there were Fe(III) (oxyhydr)oxides with lower MS, such as lepidocrocite or goethite, transformed from Fh when the initial Fe(II)/Fe(III) is too low (lower than 0.5) to initiate nucleation of magnetite. When the initial Fe(II)/Fe(III) is high (higher than 10), the rate of reduction was so fast such that an insufficient number of nucleation sites were available to promote the formation of magnetite. However, in biotic batch reactors, the total Fe(II)/Fe(III) ratio for aFh was much lower (0.29) when magnetite was produced, implying the strong influence of bacteria on magnetite transformation.

Role of *S. oneidensis* in Fh Transformation. Although bacteria can initiate nucleation of magnetite at low Fe(II) concentration based on the results of final mineral product percentages (Figure 4), the transformations of aFh, bFh-bleach, and aFh-HA to magnetite were restricted within the biotic systems compared to the abiotic systems. For instance, the relative amounts of magnetite formed in aFh, bFh-bleach, and aFh-HA were lower in biotic systems than in abiotic systems (based on Mössbauer spectroscopy data). In biotic systems, magnetite precipitation is catalyzed by the microbial reduction of Fe(III) (i.e., ferrihydrite), which leads to the release of Fe(II), which can further react with Fh to form magnetite. Previous studies have shown that the association of Fe(II) with solid phases can significantly increase the reactivity of Fe(II) because surface complexation of Fe(II) by hydroxyl groups on the mineral surface stabilizes the Fe(III) oxidation state and can decrease in the Fe(III)–Fe(II) redox potential.[37−39] In the biotic batch reactors, the reaction between Fe(III) in the solid phase and Fe(II) produced by the bacteria might be inhibited by bacterial cells (*S. oneidensis* MR-1) blocking surface sites and thus decrease the extent of Fh transformation to magnetite. The passivation of Fh and/or sequestration of Fe(II) by bacterial cells and associated biomass, such as extracellular polymeric substances (EPS), was confirmed by preliminary experiments of biotic transformation with different cell numbers. *S. oneidensis* MR-1 with a cell number of 2×10^9 cells/mL produced more $Fe(II)_{total}$ (4.25 mM; $Fe(II)_{total}$ denotes Fe(II) in aqueous and solid phases) from aFh than that with cell numbers of 1×10^9 cells/mL (3.83 mM) and 5×10^8 cells/mL (3.18 mM) (Figure S4). Additionally, Fe(II)/Fe(III) of Fh transformation with a cell number of 2×10^9 cells/mL (0.96) was higher than that with cell numbers of 1×10^9 cells/mL (0.7) and 5×10^8 cells/mL

https://dx.doi.org/10.1021/acs.est.9b07095
Environ. Sci. Technol. 2020, 54, 4121−4130

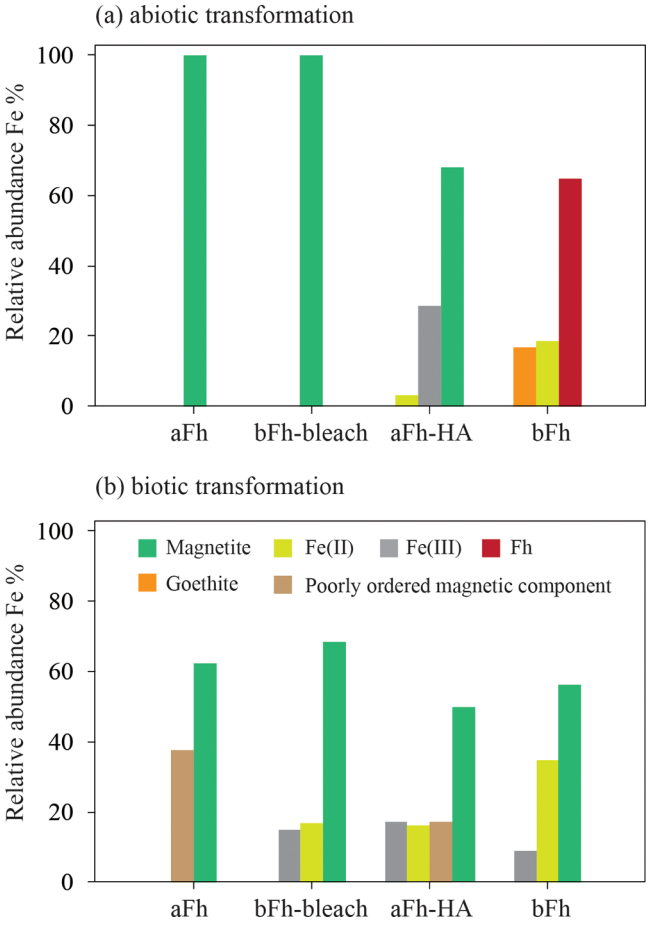

Figure 4. Percentages of transformation products from ferrihydrite induced by Fe_{aq}^{2+} abiotically (a) and *S. oneidensis* MR-1 (b).

(0.52). However, the MS of Fh transformation with a cell number of 2×10^9 cells/mL (601×10^{-6} SI) was much lower than that with cell numbers of 1×10^9 cells/mL (2928×10^{-6} SI) and 5×10^8 cells/mL (2871×10^{-6} SI). Mössbauer spectroscopy results were consistent with the above Fe concentration, which showed that 70.5 and 62.3% Fe were present as magnetite transformation products from Fh by *S. oneidensis* MR-1 with cell numbers of 1×10^9 and 5×10^8 cells/mL (Figures 3 and S5). However, it is hard to distinguish the sextet present in transformation products from Fh by *S. oneidensis* MR-1 with a cell number of 2×10^9 cells/mL, which is due to either goethite or magnetite and due to poor signal-to-noise ratio. This undefined sextet corresponds to up to 25% Fe present. Therefore, biotic transformation results with different cell numbers suggested bacterial cells and associated biomass, such as EPS, adsorbed/complexed Fe(II), and potentially passivated Fh surface, and hindered the reaction between Fh and Fe(II). A similar effect has been observed when Fh was inoculated with Fe(III)-reducing bacteria, resulting in a decrease of the transformation rate for Fh and spatial heterogeneity of the secondary mineralization products compared to abiotic Fh transformation.[40−43] Additionally, a previous study which explored the effect of a dissolved organic exudate released by Fe(III)-reducing bacteria on the kinetics of Fh transformation (by isolation of the exudate containing Fe(II)) showed that the presence of the bacteria cells, and not the exudate alone, hinders the transformation rates of Fh to secondary minerals.[40]

Delay between Reduction and Magnetite Formation (Δt). There is a clear lag between the increase of Fe(II)/Fe(III) ratio and the increase of MS for aFh-HA, bFh, and bFh-bleach during biotic transformation (Figure 5). This suggests a delay in the order of days to months between the production of Fe(II) by biotic Fe(III) reduction and the precipitation of magnetite. The averaged triplicate values of Fe(II)/Fe(III) ratios in the solids and MS average were fitted with the Hill equation, which provided a close approximation to the data (see the Supporting Information). The first-order derivative of the respective model was then calculated to provide information related to the rates of Fe(III) reduction and magnetite formation. The fastest rate of Fe(II)/Fe(III) or MS increase was determined from the maxima of the respective first-order derivatives (Figure 5, Table S4). We refer to the difference between the maximum rate of Fe(II)/Fe(III) and MS increase as Δt. There was almost no delay for the three Fh substrates (aFh, aFh-HA, bFh-bleach) which transformed to magnetite during abiotic transformations (Figure S6). In biotic transformations, aFh showed almost no delay (<1 d), while for bFh-bleach, aFh-HA, and bFh, the Δt were 19, 33, and ~40 d, respectively. We postulate that the mechanisms which are causing these delays between biotic Fe(III) reduction and magnetite formation include (i) Fh surface passivation by an organic layer and (ii) complexation of Fe(II) by bacterial cells. An organic layer formed by biomass (from the Fe(II)-oxidizing bacteria which produced the Fh) or HA can block or passivate the surface of Fh against reaction with Fe(II), resulting in no direct magnetite production. As mentioned above, bacteria cells adsorbing/complexing with Fe(II) could passivate Fe(II) and hinder the reaction between Fh and Fe(II). We postulate that over time this organic layer and bacteria cells degrade, allowing the reaction between Fe(II) and Fh and initiating transformation to magnetite. Similar results in previous studies showed the strong initial interactions between biogenic organic matter and iron with biogenic organic matter released over the course of days to weeks, eventually allowing the iron minerals to precipitate.[44−46]

Effect of HA and Biomass on the Rates and Extent of Transformation of Fh. All Fh substrates in both abiotic and biotic experiments transformed to magnetite with the exception of bFh in the abiotic experiment. bFh underwent further transformation into more thermodynamically stable goethite with no magnetite produced within 64 days in the abiotic experiment. Similar results have been found in other studies, which demonstrate that organic matter strongly retards or even suppresses Fe(II)-induced abiotic transformation of Fh when exposed to the OM-Fe coprecipitates with C/Fe molar ratios of ~0.7−4.2 at 0.2−5.0 mM Fe_{aq}^{2+}.[18−20,47−49] Here, the lower C/Fe molar ratio of bFh (0.39) and higher initial Fe_{aq}^{2+} concentration (~7 mM) compared with previous studies still appear to limit abiotic Fh transformation, implying the delaying or even inhibiting effect of biomass on Fh transformation. Although the C/Fe molar ratios of aFh-HA and bFh are similar, the extent of decrease of the Fh transformation rate by microbial biomass is much larger compared with that of HA. Even when treated with bleach to remove 97% biomass for bFh, the residual biomass or the lower surface reactivity of bFh-bleach due to the bleach treatment still delayed the Fh transformation. The possible mechanisms for the delaying or inhibiting effect of HA and biomass on Fh transformation could be the complexation of Fe(II) by OM, which can decrease free Fe_{aq}^{2+} concentration in

https://dx.doi.org/10.1021/acs.est.9b07095
Environ. Sci. Technol. 2020, 54, 4121−4130

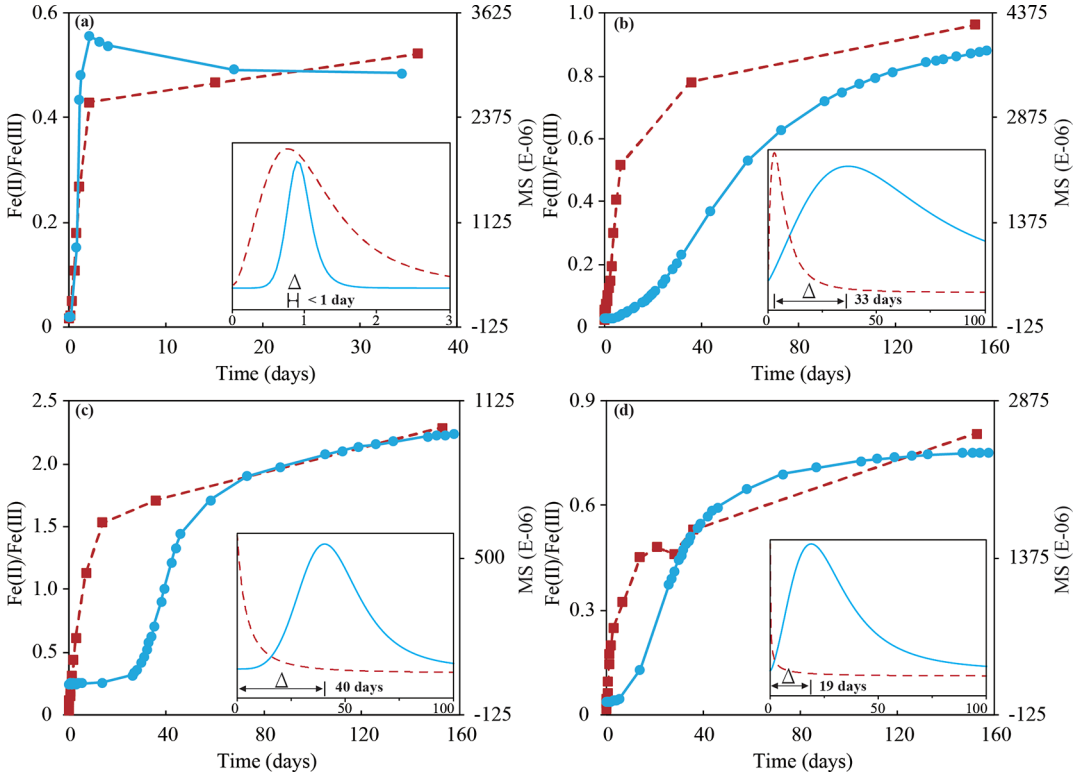

Figure 5. Fe(II)/Fe(III) compared to MS over time in biotic transformation of aFh (a), aFh-HA (b), bFh (c), and bFh-bleach (d). The red and blue lines correspond to Fe(II)/Fe(III) and MS, respectively. The insets show the first derivative of Fe(II)/Fe(III) and MS.

the solution and thus lower secondary mineral transformations of Fh.[22,50] However, based on the Fe_{aq}^{2+} concentration in our study, there was less Fe_{aq}^{2+} removal in abiotic transformation and more Fe_{aq}^{2+} in the aqueous phase of biotic transformation for Fh with OM than that without OM, suggesting that complexation of Fe(II) by OM is a minor component of our system.

Magnetite forms via solid-state conversion of Fh or via dissolution of Fh and subsequent reprecipitation and/or a combination of both.[8,51,52] For both pathways, adsorption of Fe(II) to Fh is necessary to induce electron transfer and drive the transformation.[40,53,54] Additionally, previous experimental results have also demonstrated that the microbial reduction rate and extent of Fe(III) (oxyhydr)oxides are controlled by the surface area and site concentration of the Fe(III) (oxyhydr)oxides.[22,55,56] HA and biomass partially blocked adsorption sites and therefore prevented or slowed the transformation of Fh to magnetite. The SSA results of the four Fh substrates also confirmed this assumption; the presence of HA and biomass decreased the SSA of Fh and led to the formation of larger aggregates, resulting in the lower accessible surface area per mass ferrihydrite for electron transfer. Recent studies on atom exchange between aqueous $^{57}Fe(II)$ and $^{56}Fe(II)$ with Fh-OM show that even though electron transfer still occurs between Fe(II) and Fh-OM, no measurable formation of secondary minerals can be observed.[20,57] These results imply that although OM fails to prevent the electron transfer between Fe(II) and Fh-OM, it can retard secondary mineral transformation of Fh by inhibiting Fh aggregation and growth via Ostwald ripening, thus stabilizing Fh. Alternatively, the presence of HA and biomass can induce a negative surface charge of Fh, which can block the sorption of negatively charged cells on the Fh surface because of electrostatic repulsion. In summary, both HA and biomass affect Fh mineral properties, such as sorption site availability, surface area, and mineral charge, inducing unique mineral transformation behavior for bFh and aFh-HA from aFh under abiotic and biotic reducing conditions. Additionally, the abiotic transformation products from bFh and aFh-HA were goethite and magnetite, respectively, suggesting that while the similar mechanisms for the delaying or inhibiting impact of HA and biomass on Fh transformation may be at play, the overall effect of HA versus biomass association with Fh was different.

Environmental Implications. The transformation of Fe minerals directly influences Fe cycling as well as the fate of associated nutrients and contaminants. Magnetite formation is of particular interest because of its high reactivity toward pollutants in the environment and its magnetic properties, which make it as a potential tool for climate reconstruction and organic contaminant detection.[58,59] This study advances our understanding of the formation of magnetite under different geochemical settings relevant to the environment. Our work further advances previous studies[20,22,57] which have predominantly focused on the transformation of ferrihydrite and not specifically looked at the rates of magnetite precipitation as we have investigated here. The results of our study highlight the importance of the Fe(II)/Fh ratio in the rate and extent of magnetite formation. Abiotic ferrihydrite transformation to magnetite may not occur in soils and sediments containing extremely low or high Fe(II)/Fh ratios. For example, such a scenario may be expected in the surface water that is fully oxygenated. Additionally, we hypothesized that microbial biomass associated with biogenic Fh could block or inhibit the reaction between Fh and Fe_{aq}^{2+} and stabilize Fh; however, Fh remains bioavailable even when associated with biomass, as demonstrated by the transformation to magnetite. However,

https://dx.doi.org/10.1021/acs.est.9b07095
Environ. Sci. Technol. 2020, 54, 4121−4130

although the OM-Fh coprecipitates are more stable than pure Fh in the natural environment over long periods of time, it can still undergo transformation, especially if there is a shift in the geochemical conditions. Further studies on the bonding between biomass and Fh, such as the sorption versus inclusion/occlusion into the structure, as well as the release of organic carbon and variation of magnetite particle sizes during microbial reduction of bFh, are needed to make definitive conclusions on the biogeochemical impacts of biomass on Fe cycling.

■ ASSOCIATED CONTENT

Supporting Information

The Supporting Information is available free of charge at https://pubs.acs.org/doi/10.1021/acs.est.9b07095.

Additional materials and methods, properties of four initial Fh substrates, Mössbauer spectroscopy hyperfine parameters, Fe(II)/Fe(III) ratio of each of the magnetite formation products determined based on Mössbauer spectroscopy and information for fitted lines of Fe(II)/Fe(III) and MS, outline of all batch reactors, Mössbauer spectrum of four Fh substrates, MS for abiotic transformation with different Fe(II):Fh ratios, Fe concentrations, MS and Mössbauer spectrum for biotic transformation with different cell numbers, and lag phase in abiotic transformation and Hill plots for abiotic and biotic transformation (PDF)

■ AUTHOR INFORMATION

Corresponding Author

James M. Byrne − *Geomicrobiology, Center for Applied Geosciences, University of Tuebingen, Tuebingen 72074, Germany;* orcid.org/0000-0002-4399-7336; Email: james.byrne@uni-tuebingen.de

Authors

Xiaohua Han − *Biogeomagnetism Group, Key Laboratory of Earth and Planetary Physics, Institute of Geology and Geophysics and France-China International Laboratory of Evolution and Development of Magnetotactic Multicellular Organisms, Chinese Academy of Sciences, Beijing 100029, China; Geomicrobiology, Center for Applied Geosciences, University of Tuebingen, Tuebingen 72074, Germany; College of Earth and Planetary Sciences, University of Chinese Academy of Sciences, Beijing 100049, China;* orcid.org/0000-0003-0305-2706

Elizabeth J. Tomaszewski − *Geomicrobiology, Center for Applied Geosciences, University of Tuebingen, Tuebingen 72074, Germany*

Julian Sorwat − *Geomicrobiology, Center for Applied Geosciences, University of Tuebingen, Tuebingen 72074, Germany*

Yongxin Pan − *Biogeomagnetism Group, Key Laboratory of Earth and Planetary Physics, Institute of Geology and Geophysics and France-China International Laboratory of Evolution and Development of Magnetotactic Multicellular Organisms, Chinese Academy of Sciences, Beijing 100029, China; College of Earth and Planetary Sciences, University of Chinese Academy of Sciences, Beijing 100049, China*

Andreas Kappler − *Geomicrobiology, Center for Applied Geosciences, University of Tuebingen, Tuebingen 72074, Germany;* orcid.org/0000-0002-3558-9500

Complete contact information is available at: https://pubs.acs.org/10.1021/acs.est.9b07095

Notes

The authors declare no competing financial interest.

■ ACKNOWLEDGMENTS

This research was funded by the German Research Foundation (DFG) under grant no. KA 1736/39-1. We thank China Scholarship Council (CSC) for the financial support to X.H. Y.P. was supported by a grant of the National Natural Science Foundation of China (41621004).

■ REFERENCES

(1) Usman, M.; Byrne, J. M.; Chaudhary, A.; Orsetti, S.; Hanna, K.; Ruby, C.; Kappler, A.; Haderlein, S. B. Magnetite and Green Rust: Synthesis, Properties, and Environmental Applications of Mixed-Valent Iron Minerals. *Chem. Rev.* **2018**, *118*, 3251−3304.

(2) Byrne, J. M.; Klueglein, N.; Pearce, C.; Rosso, K. M.; Appel, E.; Kappler, A. Redox cycling of Fe(II) and Fe(III) in magnetite by Fe-metabolizing bacteria. *Science* **2015**, *347*, 1473.

(3) Melton, E. D.; Swanner, E. D.; Behrens, S.; Schmidt, C.; Kappler, A. The interplay of microbially mediated and abiotic reactions in the biogeochemical Fe cycle. *Nat. Rev. Microbiol.* **2014**, *12*, 797−808.

(4) Pankhurst, Q. A.; Connolly, J.; Jones, S. K.; Dobson, J. Applications of magnetic nanoparticles in biomedicine. *J. Phys. D: Appl. Phys.* **2003**, *36*, R167−R181.

(5) Su, C. Environmental implications and applications of engineered nanoscale magnetite and its hybrid nanocomposites: A review of recent literature. *J. Hazard. Mater.* **2017**, *322*, 48−84.

(6) Byrne, J. M.; Kappler, A. Current and future microbiological strategies to remove As and Cd from drinking water. *Microb. Biotechnol.* **2017**, *10*, 1098−1101.

(7) Hansel, C. M.; Benner, S. G.; Neiss, J.; Dohnalkova, A.; Kukkadapu, R. K.; Fendorf, S. Secondary mineralization pathways induced by dissimilatory iron reduction of ferrihydrite under advective flow. *Geochim. Cosmochim. Acta* **2003**, *67*, 2977−2992.

(8) Cornell, R. M.; Schwertmann, U. *The Iron Oxides: Structure, Properties, Reactions, Occurrences and Uses*; John Wiley & Sons, 2003.

(9) Liu, H.; Li, P.; Lu, B.; Wei, Y.; Sun, Y. Transformation of ferrihydrite in the presence or absence of trace Fe(II): The effect of preparation procedures of ferrihydrite. *J. Solid State Chem.* **2009**, *182*, 1767−1771.

(10) Ruby, C.; Géhin, A.; Abdelmoula, M.; Génin, J.-M. R.; Jolivet, J.-P. Coprecipitation of Fe(II) and Fe(III) cations in sulphated aqueous medium and formation of hydroxysulphate green rust. *Solid State Sci.* **2003**, *5*, 1055−1062.

(11) Byrne, J. M.; Muhamadali, H.; Coker, V. S.; Cooper, J.; Lloyd, J. R. Scale-up of the production of highly reactive biogenic magnetite nanoparticles using Geobacter sulfurreducens. *J. R. Soc., Interface* **2015**, *12*, 20150240.

(12) Hansel, C. M.; Benner, S. G.; Fendorf, S. Competing Fe(II)-Induced Mineralization Pathways of Ferrihydrite. *Environ. Sci. Technol.* **2005**, *39*, 7147−7153.

(13) Fredrickson, J. K.; Zachara, J. M.; Kennedy, D. W.; Dong, H.; Onstott, T. C.; Hinman, N. W.; Li, S.-m. Biogenic iron mineralization accompanying the dissimilatory reduction of hydrous ferric oxide by a groundwater bacterium. *Geochim. Cosmochim. Acta* **1998**, *62*, 3239−3257.

(14) Lalonde, K.; Mucci, A.; Ouellet, A.; Gélinas, Y. Preservation of organic matter in sediments promoted by iron. *Nature* **2012**, *483*, 198.

(15) Zhao, Q.; Poulson, S. R.; Obrist, D.; Sumaila, S.; Dynes, J. J.; Mcbeth, J. M.; Yang, Y. Iron-Bound Organic Carbon in Forest Soils: Quantification and Characterization. *Biogeosciences* **2016**, *13*, 4777.

(16) Lovley, D. R. Microbial Fe(III) reduction in subsurface environments. *FEMS Microbiol. Rev.* **1997**, *20*, 305−313.

(17) Lovley, D. R.; Anderson, R. T. Influence of dissimilatory metal reduction on fate of organic and metal contaminants in the subsurface. *Hydrogeol. J.* **2000**, *8*, 77−88.
(18) Jones, A. M.; Collins, R. N.; Rose, J.; Waite, T. D. The effect of silica and natural organic matter on the Fe(II)-catalysed transformation and reactivity of Fe(III) minerals. *Geochim. Cosmochim. Acta* **2009**, *73*, 4409−4422.
(19) Chen, C.; Kukkadapu, R.; Sparks, D. L. Influence of Coprecipitated Organic Matter on Fe2+(aq)-Catalyzed Transformation of Ferrihydrite: Implications for Carbon Dynamics. *Environ. Sci. Technol.* **2015**, *49*, 10927−10936.
(20) ThomasArrigo, L. K.; Byrne, J. M.; Kappler, A.; Kretzschmar, R. Impact of Organic Matter on Iron(II)-Catalyzed Mineral Transformations in Ferrihydrite-Organic Matter Coprecipitates. *Environ. Sci. Technol.* **2018**, *52*, 12316−12326.
(21) Han, L.; Sun, K.; Keiluweit, M.; Yang, Y.; Yang, Y.; Jin, J.; Sun, H.; Wu, F.; Xing, B. Mobilization of ferrihydrite-associated organic carbon during Fe reduction: Adsorption versus coprecipitation. *Chem. Geol.* **2019**, *503*, 61−68.
(22) Shimizu, M.; Zhou, J.; Schröder, C.; Obst, M.; Kappler, A.; Borch, T. Dissimilatory Reduction and Transformation of Ferrihydrite-Humic Acid Coprecipitates. *Environ. Sci. Technol.* **2013**, *47*, 13375−13384.
(23) Eusterhues, K.; Hädrich, A.; Neidhardt, J.; Küsel, K.; Keller, T. F.; Jandt, K. D.; Totsche, K. U. Reduction of ferrihydrite with adsorbed and coprecipitated organic matter: microbial reduction by Geobacter bremensis vs. abiotic reduction by Na-dithionite. *Biogeosciences* **2014**, *11*, 4953−4966.
(24) Amstaetter, K.; Borch, T.; Kappler, A. Influence of humic acid imposed changes of ferrihydrite aggregation on microbial Fe(III) reduction. *Geochim. Cosmochim. Acta* **2012**, *85*, 326−341.
(25) Emerson, D.; Weiss, J. V. Bacterial Iron Oxidation in Circumneutral Freshwater Habitats: Findings from the Field and the Laboratory. *Geomicrobiol. J.* **2004**, *21*, 405−414.
(26) Emerson, D.; Fleming, E. J.; McBeth, J. M. Iron-Oxidizing Bacteria: An Environmental and Genomic Perspective. *Annu. Rev. Microbiol.* **2010**, *64*, 561−583.
(27) Duckworth, O. W.; Holmström, S. J. M.; Peña, J.; Sposito, G. Biogeochemistry of iron oxidation in a circumneutral freshwater habitat. *Chem. Geol.* **2009**, *260*, 149−158.
(28) Sowers, T. D.; Holden, K. L.; Coward, E. K.; Sparks, D. L. Dissolved Organic Matter Sorption and Molecular Fractionation by Naturally Occurring Bacteriogenic Iron (Oxyhydr)oxides. *Environ. Sci. Technol.* **2019**, *53*, 4295−4304.
(29) Raven, K. P.; Jain, A.; Loeppert, R. H. Arsenite and Arsenate Adsorption on Ferrihydrite: Kinetics, Equilibrium, and Adsorption Envelopes. *Environ. Sci. Technol.* **1998**, *32*, 344−349.
(30) Hegler, F.; Posth, N. R.; Jiang, J.; Kappler, A. Physiology of phototrophic iron(II)-oxidizing bacteria: implications for modern and ancient environments. *FEMS Microbiol. Ecol.* **2008**, *66*, 250−260.
(31) Lavkulich, L. M.; Wiens, J. H. Comparison of Organic Matter Destruction by Hydrogen Peroxide and Sodium Hypochlorite and Its Effects on Selected Mineral Constituents1. *Soil Sci. Soc. Am. J.* **1970**, *34*, 755−758.
(32) Stookey, L. L. Ferrozine—a new spectrophotometric reagent for iron. *Anal. Chem.* **1970**, *42*, 779−781.
(33) Rancourt, D. G.; Ping, J. Y. Voigt-based methods for arbitrary-shape static hyperfine parameter distributions in Mössbauer spectroscopy. *Nucl. Instrum. Methods Phys. Res., Sect. B* **1991**, *58*, 85−97.
(34) Porsch, K.; Dippon, U.; Rijal, M. L.; Appel, E.; Kappler, A. In-Situ Magnetic Susceptibility Measurements As a Tool to Follow Geomicrobiological Transformation of Fe Minerals. *Environ. Sci. Technol.* **2010**, *44*, 3846−3852.
(35) Dunlop, D. J.; Özdemir, Ö. *Rock Magnetism: Fundamentals and Frontiers*; Cambridge University Press, 2001; Vol. *3*.
(36) Gorski, C. A.; Scherer, M. M. Determination of nanoparticulate magnetite stoichiometry by Mossbauer spectroscopy, acidic dissolution, and powder X-ray diffraction: A critical review. *Am. Mineral.* **2010**, *95*, 1017−1026.
(37) Pecher, K.; Haderlein, S. B.; Schwarzenbach, R. P. Reduction of Polyhalogenated Methanes by Surface-Bound Fe(II) in Aqueous Suspensions of Iron Oxides. *Environ. Sci. Technol.* **2002**, *36*, 1734−1741.
(38) Elsner, M.; Schwarzenbach, R. P.; Haderlein, S. B. Reactivity of Fe(II)-Bearing Minerals toward Reductive Transformation of Organic Contaminants. *Environ. Sci. Technol.* **2004**, *38*, 799−807.
(39) Stumm, W.; Sulzberger, B.; Sinniger, J. The coordination chemistry of the oxide-electrolyte interface; the dependence of surface reactivity (dissolution, redox reactions) on surface structure. *Croat. Chem. Acta* **1990**, *63*, 277−312.
(40) Xiao, W.; Jones, A. M.; Li, X.; Collins, R. N.; Waite, T. D. Effect of Shewanella oneidensis on the Kinetics of Fe(II)-Catalyzed Transformation of Ferrihydrite to Crystalline Iron Oxides. *Environ. Sci. Technol.* **2018**, *52*, 114−123.
(41) Pallud, C.; Kausch, M.; Fendorf, S.; Meile, C. Spatial Patterns and Modeling of Reductive Ferrihydrite Transformation Observed in Artificial Soil Aggregates. *Environ. Sci. Technol.* **2010**, *44*, 74−79.
(42) Pallud, C.; Masue-Slowey, Y.; Fendorf, S. Aggregate-scale spatial heterogeneity in reductive transformation of ferrihydrite resulting from coupled biogeochemical and physical processes. *Geochim. Cosmochim. Acta* **2010**, *74*, 2811−2825.
(43) Dippon, U.; Schmidt, C.; Behrens, S.; Kappler, A. Secondary Mineral Formation During Ferrihydrite Reduction byShewanella oneidensisMR-1 Depends on Incubation Vessel Orientation and Resulting Gradients of Cells, Fe2+and Fe Minerals. *Geomicrobiol. J.* **2015**, *32*, 878−889.
(44) Adhikari, D.; Zhao, Q.; Das, K.; Mejia, J.; Huang, R.; Wang, X.; Poulson, S. R.; Tang, Y.; Roden, E. E.; Yang, Y. Dynamics of ferrihydrite-bound organic carbon during microbial Fe reduction. *Geochim. Cosmochim. Acta* **2017**, *212*, 221−233.
(45) Pan, W.; Kan, J.; Inamdar, S.; Chen, C.; Sparks, D. Dissimilatory microbial iron reduction release DOC (dissolved organic carbon) from carbon-ferrihydrite association. *Soil Biol. Biochem.* **2016**, *103*, 232−240.
(46) Chan, C. S.; Fakra, S. C.; Edwards, D. C.; Emerson, D.; Banfield, J. F. Iron oxyhydroxide mineralization on microbial extracellular polysaccharides. *Geochim. Cosmochim. Acta* **2009**, *73*, 3807−3818.
(47) Pasakarnis, T. S. Effects of carbon during Fe (II)-catalyzed Fe oxide recrystallization: implications for Fe and carbon cycling. Ph.D. Thesis, The University of Iowa, 2013.
(48) Henneberry, Y. K.; Kraus, T. E. C.; Nico, P. S.; Horwath, W. R. Structural stability of coprecipitated natural organic matter and ferric iron under reducing conditions. *Org. Geochem.* **2012**, *48*, 81−89.
(49) Xiao, W.; Jones, A. M.; Collins, R. N.; Waite, T. D. Investigating the effect of ascorbate on the Fe(II)-catalyzed transformation of the poorly crystalline iron mineral ferrihydrite. *Biochim. Biophys. Acta, Gen. Subj.* **2018**, *1862*, 1760−1769.
(50) ThomasArrigo, L. K.; Mikutta, C.; Byrne, J.; Kappler, A.; Kretzschmar, R. Iron(II)-Catalyzed Iron Atom Exchange and Mineralogical Changes in Iron-rich Organic Freshwater Flocs: An Iron Isotope Tracer Study. *Environ. Sci. Technol.* **2017**, *51*, 6897−6907.
(51) Tronc, E.; Belleville, P.; Jolivet, J. P.; Livage, J. Transformation of ferric hydroxide into spinel by iron(II) adsorption. *Langmuir* **1992**, *8*, 313−319.
(52) Bazylinski, D. A.; Frankel, R. B.; Konhauser, K. O. Modes of Biomineralization of Magnetite by Microbes. *Geomicrobiol. J.* **2007**, *24*, 465−475.
(53) Jolivet, J. P.; Belleville, P.; Tronc, E.; Livage, J. Influence of Fe(II) on the Formation of the Spinel Iron Oxide in Alkaline Medium. *Clays Clay Miner.* **1992**, *40*, 531−539.
(54) Elisabeth, T.; Philippe, B.; Jolivet, J.-P. Transformation of Ferric Hydroxide Into Spinel by Fell Adsorption [J]. *Langmuir* **1992**, *8*, 313.
(55) Roden, E. E.; Zachara, J. M. Microbial Reduction of Crystalline Iron(III) Oxides: Influence of Oxide Surface Area and Potential for Cell Growth. *Environ. Sci. Technol.* **1996**, *30*, 1618−1628.

https://dx.doi.org/10.1021/acs.est.9b07095
Environ. Sci. Technol. 2020, 54, 4121−4130

(56) Roden, E. E. Fe(III) Oxide Reactivity Toward Biological versus Chemical Reduction. *Environ. Sci. Technol.* **2003**, *37*, 1319−1324.
(57) Zhou, Z.; Latta, D. E.; Noor, N.; Thompson, A.; Borch, T.; Scherer, M. M. Fe(II)-Catalyzed Transformation of Organic Matter-Ferrihydrite Coprecipitates: A Closer Look Using Fe Isotopes. *Environ. Sci. Technol.* **2018**, *52*, 11142−11150.
(58) Porsch, K.; Rijal, M. L.; Borch, T.; Troyer, L. D.; Behrens, S.; Wehland, F.; Appel, E.; Kappler, A. Impact of organic carbon and iron bioavailability on the magnetic susceptibility of soils. *Geochim. Cosmochim. Acta* **2014**, *128*, 44−57.
(59) Ahmed, I. A. M.; Maher, B. A. Identification and paleoclimatic significance of magnetite nanoparticles in soils. *Proc. Natl. Acad. Sci. U.S.A.* **2018**, *115*, 1736−1741.

https://dx.doi.org/10.1021/acs.est.9b07095
Environ. Sci. Technol. 2020, 54, 4121−4130